QUANTUM CORRELATIONS AND FISHER INFORMATION IN MULTIPARTITE TWO-LEVEL SYSTEM UNDER KERR MEDIUM EFFECT

by

Shaimaa ALMALKI[a], Muhammad IBRAHIM[b], S. Jamal ANWAR[b*], Muhammad ILYAS[b], Sayed ABDEL KHALEK[c], Tahani M. ALBOGAMI[d], and M. Khalid KHAN[b]

[a] Department of Physics, Najran University, Najran, Saudi Arabia
[b] Department of Physics, Quaid-i-Azam University, Islamabad, Pakistan
[c] Department of Mathematics, College of Science, Taif University, Taif, Saudi Arabia
[d] Department of Physical Science, Faculty of Science, University of Jeddah, Jeddah, Saudi Arabia

Original scientific paper
https://doi.org/10.2298/TSCI2501347A

This paper investigates the evolution of global quantum discord (GQD) and quantum Fisher information (QFI) of the interaction of multiple two-level atomic systems (TLS) with a single thermal field mode and a non-linear Kerr medium (NLKM) considering the cases of intrinsic decoherence and its absence. Results indicate that increasing the number of atomic systems (N) while maintaining the NLKM parameter constant χ leads to higher GQD and QFI values for both intrinsic intrinsic decoherence cases. With rising χ, the GQD values decrease but the oscillation rate of the GQD increases. The presence of intrinsic decoherence does not significantly reduce the GQD quasi-static value compared to the no-decoherence scenario for certain χ values. At the same time, a different trend is observed for higher χ values. The average QFI value rises with reduced oscillation amplitudes for higher χ values and larger N subsystems. Unlike the GQD, higher χ values aid in maintaining average QFI in the presence of intrinsic decoherence. For moving TLS, changing χ does not alter the oscillation periods of the GQD and QFI. The GQD values decrease with increased χ in the moving system case, while the QFI improves with higher χ values. Additionally, higher average thermal photons within the system suppress the GQD and QFI values and decrease oscillation amplitudes for both quantifiers.

Key words: *GQD, QFI, quantum entanglement, multipartite quantum system, NLKM, Tavais-Cumming model, intrinsic decoherence*

Introduction

In quantum mechanics, two atoms can achieve entanglement through non-linear, non-degenerate two-photon interactions with a two-mode thermal field. Quantum entanglement between two qubits can be facilitated by interactions involving one or two modes, especially when dipole-dipole interactions are at play [1]. This phenomenon is essential in quantum information science, where numerous applications depend on reliable methods for creating entangled states. Techniques for achieving entanglement include utilizing spins in solid-state systems, superconducting circuits, or neutral atoms and ions held within cooled, confined environments such as cavities. Many applications also require maximally entangled states for optimal functional-

* Corresponding author, e-mail: sjamalanwar@gmail.com

ity. However, maintaining these pure entangled states is challenging due to decoherence, often resulting from a quantum system's interaction with its environment or non-classical processes like entanglement. Addressing the quantum entanglement of mixed states remains a key area of research in quantum information. Studies such as those by Kim *et al*. [2] have examined entanglement between two identical TLS undergoing one-photon transitions due to a single-mode thermal field, demonstrating that initially unentangled atoms can become entangled in a chaotic field with minimal information. Zhang [3] expanded on Kim's work by analyzing cases where atoms are slightly phase-shifted relative to the thermal field, exploring the implications for atom-atom quantum entanglement. Zhou *et al*. [4] explored non-linear two-photon interactions with a single-mode thermal field, showing that entanglement induced by non-linear interactions surpasses that from linear ones. Further studies on quantum entanglement driven by thermal fields are discussed in [5-7]. The interaction between a TLS and a radiation field represents the most straightforward problem in matter-radiation coupling. This interaction was first modeled by Jaynes and Cummings [8]. Later, this model was extended to account for the interaction between a four-level atom and a single quantized mode of the radiation field, incorporating the rotating wave approximation (RWA) [9]. Theoretical studies have since justified the need to consider atomic motion's impact on the Jaynes-Cummings model (JCM), with researchers using both analytical and numerical methods to explore this [10-12]. A notable outcome of these interactions is quantum entanglement [13], a cornerstone that sets quantum information theory apart from classical theories. Quantum entangled states are fundamental to quantum computation, quantum communication [14], quantum information processing [15-17], and quantum cryptography [18,19]. In quantum information, measures such as von Neumann entropy are often used to quantify quantum entanglement. The time evolution of field entropy provides insight into quantum entanglement degree over time. The dynamics of a four-level atom interacting with a single radiation field mode in a lossless cavity have been explored from multiple perspectives [20-22], with further extensions considering atomic motion and field mode structure [23]. The JCM has been expanded and adapted across various fields, including research on multi-atom interactions, multi-mode fields, Stark shifts, and Kerr non-linearity [24, 25].

The Cramer-Rao inequality establishes limits on the precision of parameter estimation in quantum measurements, while QFI plays a central role in quantum metrology and estimation theory. The QFI effectively measures how distinguishable parameters are when encoded in quantum states, thus serving as a key metric for estimation accuracy [26-29].

Milburn [30] developed an intrinsic decoherence model that posits a quantum system evolves via a stochastic sequence of identical unitary transformations over brief time intervals. This model introduces a slight modification the traditional Schrodinger equation, which, in turn, influences the von Neumann equation governing the density operator of the system. In Milburn's framework, the structure of the energy eigenstate basis naturally reduces the off-diagonal components of the density operator, achieving intrinsic decoherence without the typical dissipation associated with standard decay. The degradation observed is influenced only by phase.

Bipartite quantum discord has been widely extended to multipartite states to effectively quantify quantum correlations in larger systems [31, 32]. A measure known as GQD is introduced in [33] as a symmetric generalization of bipartite discord, designed specifically to assess quantum correlations in multipartite scenarios [33-36].

The primary focus of this paper is to examine the dynamics of QFI and quantum entanglement in a multi-TLS system interacting with a thermal field within an NLKM. We calculate both the GQD and QFI for the multi-TLS set-up, considering cases with and without intrinsic decoherence.

Quantum Fisher information

The classical Fisher information (CFI) for each distinct occurrence with one unknown parameter θ can be articulated:

$$I_{\Phi} = \sum_j \left[\frac{1}{p_j(\theta)} \frac{\partial p_j(\theta)}{\partial \theta} \right]^2 p_i(\theta) \tag{1}$$

In the aforementioned equation the probability density $p_j(\theta)$ signifies the substantial and evident impact of the fixed parameter on the measurement outcome $\{x_j\}$ for a certain observable X. The CFI can be defined as the inverse variance of the asymptotic normality of a maximum-likelihood estimator. In quantum metrology, the QFI serves a vital and beneficial function. It can be employed for the precise measurement of an unknown parameter [37], which is associated with the inverse of the QFI.

The QFI in terms of the symmetric logarithmic derivative (SLD) D and density matrix (DM) $\rho(\theta)$can be provided:

$$F_{\Phi} = \mathrm{Tr}\left[\rho(\theta) D^2 \right] \tag{2}$$

where D is the substantiates the subsequent equation:

$$2\frac{\mathrm{d}\rho(\theta)}{\mathrm{d}\theta} = D\rho(\theta) + \rho(\theta)D \tag{3}$$

The DM spectral decomposition is defined:

$$\rho_{\theta} = \sum_K \lambda_K |k\rangle\langle k| \tag{4}$$

According to eq. (4), the QFI corresponding to θ is denoted by [38]:

$$F_{\theta} = 2\sum_{k,k'} \frac{(\lambda_k - \lambda_{k'})^2}{\lambda_k + \lambda_{k'}} \left| \left\langle k \left| \frac{\partial}{\partial \theta} k' \right\rangle \right|^2 + \sum_k \frac{1}{\lambda_k} \left(\frac{\partial \lambda_k}{\partial \theta} \right)^2 \tag{5}$$

where $\lambda_k > 0$ and $\lambda_k + \lambda_{k'} > 0$. The first (second) term indicate the QFI (CFI). The trace over the field is used to calculate the atomic-QFI. Consequently, we will be able to articulate the atomic QFI of the associated bipartite density operator ρ_{AB} as [39]:

$$I_{QF}(t) = I_{AB}(\theta, t) = \mathrm{Tr}\left[\rho_{AB}(\theta, t) \left\{ D(\theta, t) \right\}^2 \right] \tag{6}$$

where $D(\theta, t)$ is the designs the SLD of the quantum score [40], which will be represented:

$$\frac{\partial \rho_{AB}(\theta, t)}{\partial \theta} = \frac{1}{2}\left[D(\theta, t)\rho_{AB}(\theta, t) + \rho_{AB}(\theta, t)D(\theta, t) \right] \tag{7}$$

Model dynamics and wavefunction

We explore the Tavais-Cumming (TC) model [41], which has been extensively analyzed and holds potential for application in multipartite quantum systems. For two identical TLS A and B interacting with a single-mode field, the TC Hamiltonian is provided in [41]. Here, we investigate the model to incorporate a cavity filled with NLKM and move two, three, and four TLS. The 3rd-order non-linear polarizability of a non-linear media is a component of the non-linear Kerr effect. The field displays a phase shift that is intensity-dependent during this process. The Kerr medium's refractive index is inversely correlated with the strength of the field:

$$n = n_0 + n_2 E^2 \tag{8}$$

where n_2 is the Kerr constant and the typical refractive index of a weak field is, and n_2 indicates how quickly the refractive index changes with optical intensity. Under the rotating wave approximation (RWA) and in the presence of the NLKM, the total TC Hamiltonian of stationary N-TLS interacting with electromagnetic field $\hat{H}_T$ [42] can be expressed:

$$\hat{H}_T = \frac{\omega_0}{2}\sum_{j=1}^{N}\hat{\sigma}_j^z + \omega\hat{a}^\dagger\hat{a} + g\sum_{j=1}^{N}\left(\hat{a}\hat{\sigma}_j^+ + \hat{a}^\dagger\hat{\sigma}_j^-\right) + \chi\left(\hat{a}^\dagger\hat{a}\right)^2 \tag{9}$$

where $\hat{a}$ ($\hat{\sigma}_j^-$) and $\hat{a}^+$ ($\hat{\sigma}_j^+$) are the annihilation (lowering) and creation (raising) operators of the cavity field (j^{th} TLS), respectively, and the inversion operator of the atomic system is. The field and atomic transition frequencies are ω_0 and ω, respectively. The multi-TLS-field coupling is represented by g. The Kerr effect is described by the parameter χ, where χ is the Kerr parameter. The TLS is moving through a cavity of length, L, at a velocity of v, so eq. (9) will then become:

$$\hat{H}_T = \frac{\omega_0}{2}\sum_{j=1}^{N}\hat{\sigma}_j^z + \omega\hat{a}^\dagger\hat{a} + \Omega(t)\sum_{j=1}^{N}\left(\hat{a}\hat{\sigma}_j^+ + \hat{a}^\dagger\hat{\sigma}_j^-\right) + \chi\left(\hat{a}^\dagger\hat{a}\right)^2 \tag{10}$$

where $\Omega(t)$ is the cavity field mode's shape function that describes the impact of the motion of the TLS:

$$\Omega(t) = \begin{cases} g\sin\left(\dfrac{\mu\pi vt}{L}\right) & \text{for} \quad \mu \neq 0 \\ g \quad \text{for } \mu = 0 \end{cases} \tag{11}$$

where μ is the parameter for atomic motion is connected with the half wavelengths and the probability distribution of the atom within the cavity. Assuming that the atom speed is $v = gL/\pi$, this results:

$$\Omega_1(t) = \int_0^t \Omega(\tau)\,\mathrm{d}\tau = \begin{cases} \dfrac{1}{\mu}\left[1 - \cos\left(\dfrac{\mu\pi vt}{L}\right)\right] & \text{for } \mu \neq 0 \\ gt \quad \text{for } \mu = 0 \end{cases} \tag{12}$$

The TLS in the cavity moves in a sinusoidal manner by Ω in contrast to gt which is the static situation. We examine the system constituted by the interaction of a single-mode thermal field with an initial mixed state of N-TLS.

The atomic-field system can be stated as pure and mixed states that are being investigated for their effects on the evolution of the quantifiers:

$$\hat{\rho}(0) = \hat{\rho}_f(0) \otimes \left[(1-p)|\psi\,\psi| + p|g_1 g_2 \ldots\ldots g_N\; g_1 g_2 \ldots\ldots g_N|\right] \tag{13}$$

where the parameter for the statistical mixture is p with $0 \leq p \leq 1$ and $|g_j\rangle$ and $|ej\rangle$ being, respectively, the atomic system's ground and ex-cited states. The formula for the ket vector:

$$|\psi\rangle = \cos(\theta)|g_1 g_2 \ldots g_N\rangle + \sin(\theta)\,|e_1 e_2 \ldots e_N\rangle$$

where $0 \leq \theta \leq \pi$. The parameter θ in $|\psi\rangle$ facilitates the analysis of how quantifiers are influenced by the superposition of atomic states. The $\rho_f(0)$ is the state of the input thermal field which is given:

$$\rho_f(0) = \sum_{n=0}^{\infty} P(n)|n\,n| \tag{14}$$

The weight function is described:

$$P(n) = \overline{n}^{n}(\overline{n}+1)^{-n-1} \tag{15}$$

where $|n\rangle$ is the Fock state. The average photon number is represented:

$$\overline{n} = 1/\frac{e^{\hbar\omega_f}}{k_B T - 1}$$

where k_B is the Boltzmann constant, ω_f – the frequency of the cavity mode, and T – the temperature.

The set of acceptable basis states $\{|\psi_i\rangle\}$ can be expressed:

$$\{|\psi_i\rangle\} = |g_1 g_2 .....g_N, n+N\rangle, |e_1 g_2 .....g_N, n+N-1\rangle, ..., |e_1 e_2 .....e_N, n\rangle \tag{16}$$

The final state of the system at time, t, becomes:

$$\hat{\rho}_{AF}(t) = \sum_{i,j}^{N} |\psi_i\rangle\langle\psi_i|\hat{\rho}(t)|\psi_j\rangle\langle\psi_j| \tag{17}$$

where $\hat{\rho}(t)$ can be expressed in terms of the initial states' eigenvalues:

$$\hat{\rho}_{AF}(t) = \sum_{i,j}^{N} \exp\left(-i(E_i - E_j)t\right) \times \langle\psi_i|\hat{\rho}(0)|\psi_j\rangle |\psi_i\rangle\langle\psi_j| \tag{18}$$

with E_m and $|\psi_m\rangle$ ($m = i, j$) design the eigenvalues and eigenvectors of the density matrix at $t = 0$. After tracing the field over the state of the system, the final state of the atomic system is achieved *i.e.*:

$$\hat{\rho}_T(t) = \mathrm{Tr}_{\mathrm{F}}\left[\hat{\rho}_{\mathrm{AF}}(t)\right]$$

In terms of intrinsic decoherence, the density matrix can be given by [43]:

$$\hat{\rho}(t) = \sum \exp\left[\frac{\gamma t}{2}(E_i - E_j)^2 - i(E_i - E_j)t\right] \times \langle\Psi_i|\hat{\rho}(0)|\Psi_j\rangle |\Psi_i\rangle\langle\Psi_j| \tag{19}$$

and E_i, E_j and $|\psi_i\rangle$, $|\psi_j\rangle$ are the eigenvalues and eigenvectors of $\hat{\rho}(t)$.

In order to calculate the quantum correlations in our multipartite system we can use the form of the GQD [44] that is given:

$$GQD(\rho_T) = \left\{ \min_{\Pi^k} \left| \left\{ \sum_{j=1}^{N} \sum_{l=0}^{1} \tilde{\rho}_j^{ll} \widetilde{\log_2 \rho_j}^{ll} - \sum_{k=0}^{N-1} \tilde{\rho}_T^{kk} \widetilde{\log_2 \rho_T}^{kk} \right\} \right. + \sum_{j=1}^{N} S(\rho_j) - S(\rho_T) \tag{20}$$

where

$$\tilde{\rho}_T^{kk} = \langle k|\hat{R}^t \rho_T \hat{R}|k\rangle \text{ and } \tilde{\rho}_j^{ll} = \langle l|\hat{\rho}_j|l\rangle \text{ and } \Pi^k = \hat{R}|k\rangle\langle k|\hat{R}^t \tag{21}$$

where $|k\rangle$ is the eigenstates of $\otimes_{j=1}^{N}\hat{\sigma}_j^z$ and $\hat{R}$ – the local qubit rotational operator acting on the j^{th} qubit and expressed as:

$$\hat{R} = \otimes_{j=1}^{N} \hat{R}_J(\varphi_j, \varphi_j) \tag{22}$$

with

$$\hat{R}_j(\theta_j, \varphi_j) = \cos\theta_j \hat{1} + i\sin\varphi_j \cos\varphi_j \hat{\sigma}_y + i\sin\varphi \sin\varphi_j \hat{\sigma}_x \tag{23}$$

Discussions of numerical results

For N-TLS ($N = 2$, 3, and 4), we analyze the dynamic behavior of the GQD and QFI. The N-TLS is interacting with the thermal field where decoherence effects are also present. An NLKM of parameter, χ, is used to fill the cavity. We have numerically obtained the dynamics of the system with a 0.01-time step size.

Figure 1 illustrates the behavior of entanglement metrics for systems with two, three, and four TLS (two-level systems) in a NLKM under conditions where $\chi = 0.3$, both with and without intrinsic decoherence. The average thermal photon level is set at $|\alpha|^2 = 3$, with the system's initial state being a mixed state with a statistical probability of $p = 0.5$ and an initial parameter $\theta = 3\pi/4$. The QFI is calculated numerically based on the initial state parameter θ. For $\gamma = 0$, the magnitude of the GQD increases as the number of TLS, N, grows. This indicates that larger N values sustain stronger non-classical correlations and quantum entanglement, with the amplitude of quantum oscillations in GQD rising accordingly. However, the behavior of QFI does not show a clear increase with additional TLS. A minor enhancement is observed for $N = 3$ and compared to $N = 2$, particularly early in scaled time for $N = 4$. As time progresses, QFI variation stabilizes for $N = 3$ and $N = 4N$, remaining largely consistent.

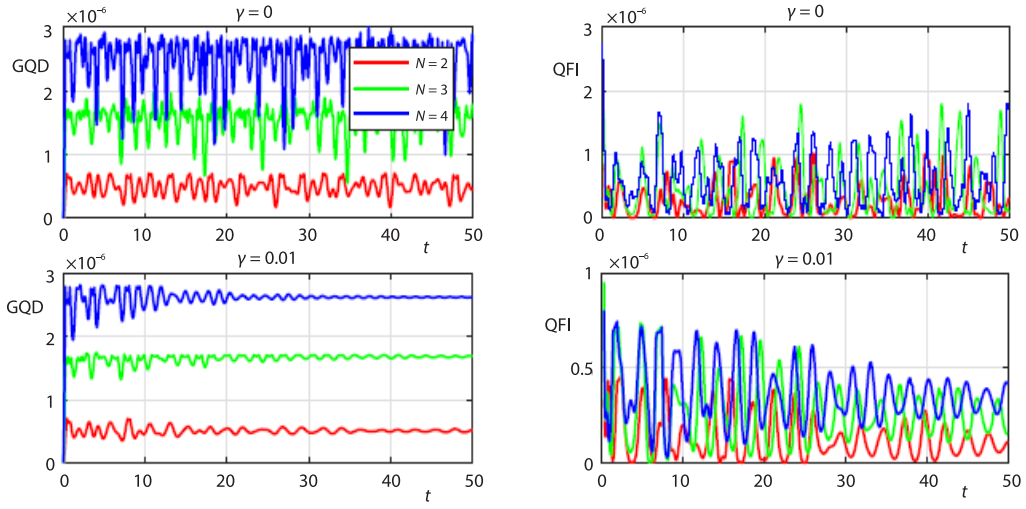

Figure 1. The dynamics of the quantifiers are shown in the figure; we have chosen the parameters $\bar{n} = 3$, $\theta = 3\pi/4$, $p = 0.5$ and the other parameters as $(\mu, \chi) = (0, 0, 3)$

Further, intrinsic decoherence, GQD and QFI exhibit nearly equivalent quantum correlations and information content for $N = 2$ and $N = 3$, while $N = 4$ shows a significant rise in quantum correlations. Initially, GQD starts at zero and then increases, whereas QFI begins at a maximum and gradually declines. Additionally, QFI demonstrates several zero crossings as time advances. When considering intrinsic decoherence with a strength of $\gamma = 0.01$, the quantifier oscillations reduce. For GQD, the quantum correlations reach a quasi-steady-state, and the magnitude of this steady-state remains unaffected by intrinsic decoherence across different N values. In contrast, both the amplitude and oscillations of QFI are suppressed in the presence of intrinsic decoherence, and these oscillations decay more slowly than those of GQD, requiring more time to reach a quasi-steady-state. Under zero-intrinsic decoherence conditions, however, QFI displays a general decreasing trend.

Figure 2 depicts the evolution of the QFI and GQD within a system in an NLKM with $\chi = 1$. When $\gamma = 0$, the GQD behavior resembles that shown in fig. 1: both its magnitude and oscillation amplitude grow as N (the number of two-level systems, or TLS) increases. In contrast, while the QFI value rises with increasing N, its oscillation amplitude decreases. For $\gamma = 0.01$, the oscillations of both quantifiers diminish over time, with the GQD oscillations decaying more rapidly than those of the QFI. The GQD's decay rate remains relatively constant as N changes, whereas for the QFI, oscillation decay accelerates with larger N values. When comparing the cases with and without intrinsic decoherence, the GQD values are largely unaffected by the intrinsic decoherence, while the QFI values decrease in the presence of intrinsic decoherence.

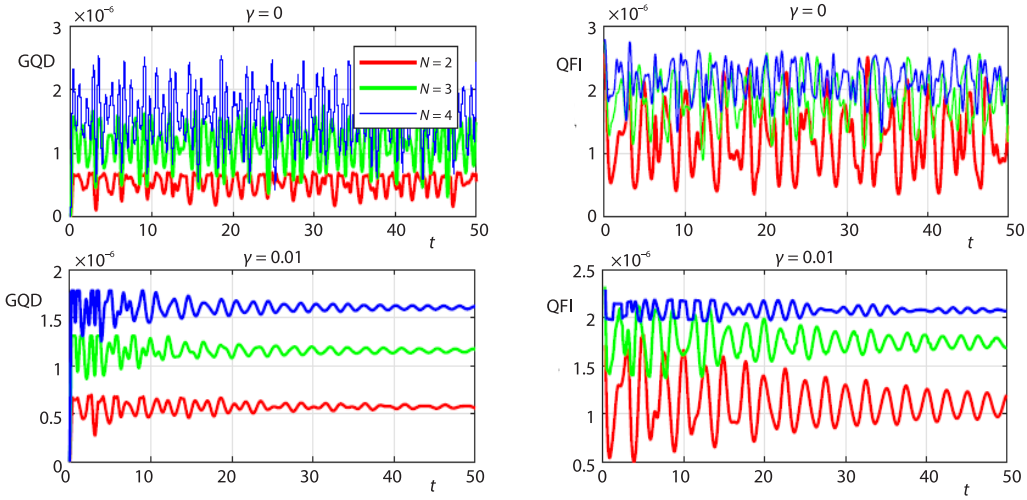

Figure 2. The dynamics of the quantifiers are shown in the figure; we have chosen the parameters $\bar{n} = 3$, $\theta = 3\pi/4$ and the other parameters as $(\mu, \chi) = (0, 1)$

Figure 3 illustrates the evolution of GQD and QFI in a system under an NLKM with $\chi = 3$. When $\gamma = 0$, both the GQD value and its amplitude show a slight increase as the number of two-level systems, N, rises. The QFI values also grow with N, but their oscillation amplitude is significantly reduced. In the $\gamma = 0.01$ scenario, oscillations in both quantifiers gradually diminish over time. GQD, in particular, smoothly decays to a quasi-static value. Comparing $\gamma = 0$ and $\gamma = 0.01$, we see a reduction in GQD with intrinsic decoherence, and the oscillation amplitude increases with N. QFI oscillations also decrease with $\gamma = 0.01$, as both QFI value and oscillation amplitude lessen with larger N. The overall dynamics of GQD and QFI with varying χ and γ values are summarized in figs. 1-3. For $\gamma = 0$, increasing χ results in lower GQD values across all N, especially pronounced in systems with $N = 3$ and $N = 4$, and faster oscillations for GQD. Under intrinsic decoherence, GQD's quasi-static value remains stable at $\chi = 0.3$ and $\chi = 1$ compared to the no-intrinsic decoherence case but reduces for $\chi = 3$ with $\gamma = 0.01$. Meanwhile, for $\gamma = 0$, the average QFI increases with higher χ, though its oscillation amplitude decreases across all N. This effect is especially evident in $N = 4N$ systems, where oscillation suppression is stronger than in $N = 2N$ and $N = 3N$ systems. With intrinsic decoherence present, the QFI average decreases at $\chi = 0.3$ relative to $\gamma = 0$, while at $\chi = 1$ and $\chi = 3$, it remains consistent across both γ cases, with more suppressed oscillations for $N = 4N$. A comparison of GQD and QFI across different χ and γ values reveals key insights. With $\gamma = 0$, GQD's average value decreases as rises, while QFI's average value increases with a larger χ. The quasi-static GQD values are further suppressed as χ grows, while QFI values show improvement with increased χ.

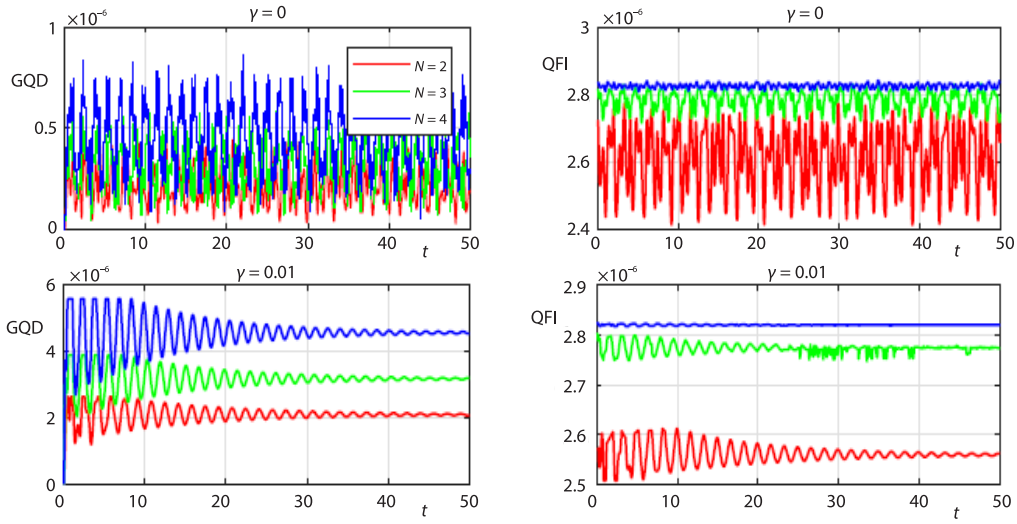

Figure 3. The dynamics of the quantifiers are shown in the figure; we have chosen the parameters $\bar{n} = 3$, $\theta = 3\pi/4$ and the other parameters as $(\mu, \chi) = (0, 3)$

To examine the dynamics of GQD and QFI in the presence of an NLKM and a thermal field, we study a moving atomic system. Figure 4 illustrates this behavior with $\chi = 0.3$, using parameters $p = 0.5$, $\theta = 3\pi/4$, and average thermal photons $|\alpha|^2 = 3$, starting from a mixed initial state. The GQD dynamics reveal periodic oscillations for both $\gamma = 0$ and $\gamma = 0.01$ across all values of N. The presence of intrinsic decoherence does not influence GQD in this configuration, and the periodic zero-point decay and increased oscillation amplitude in GQD become more pronounced with larger N. The QFI also shows periodic behavior in the presence of atomic motion, with peak values remaining the same across N values when $\gamma = 0$. However, under $\gamma = 0.01$, QFI values are suppressed relative to the zero-intrinsic decoherence scenario. Notably, maxima in GQD align with minima in QFI. For $\chi = 1$ and $\chi = 3$, represented in figs. 5 and 6, the GQD retains its periodic behavior across both γ cases. No significant reduction in GQD value is observed under $\gamma = 0.01$ compared to $\gamma = 0$, and minima appear consistently across all N values. The GQD value rises with N, and QFI maintains a periodic trend for both γ settings, with peak QFI values con-

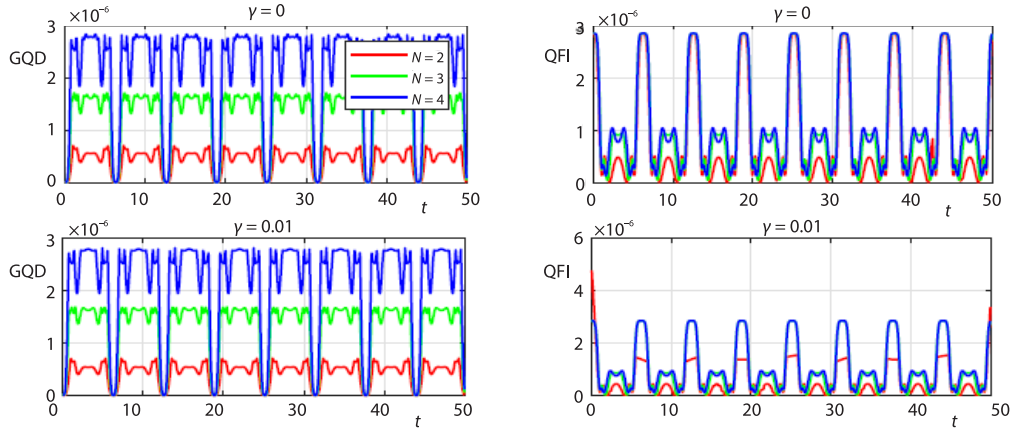

Figure 4. The dynamics of the quantifiers are shown in the figure; we have chosen the parameters $\bar{n} = 3$, $\theta = 3\pi/4$, and the other parameters as $(\mu, \chi) = (1, 0, 3)$

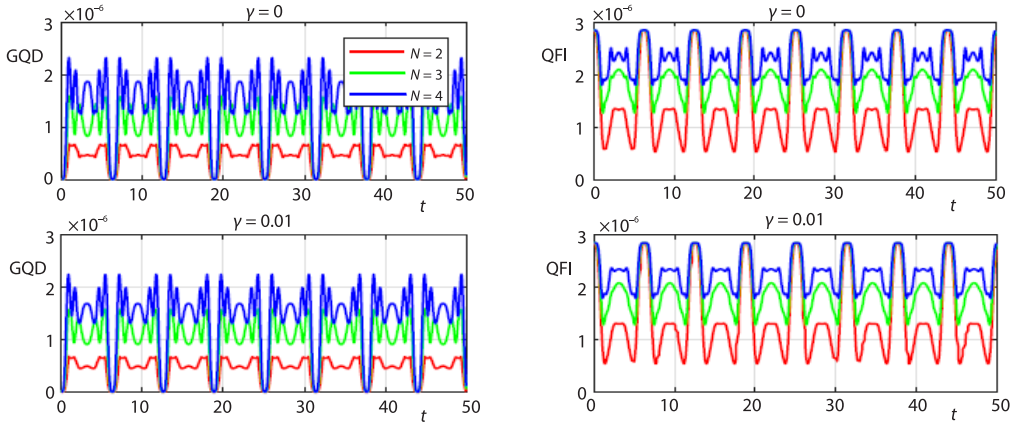

Figure 5. The dynamics of the quantifiers are shown in the figure; we have chosen the parameters $\bar{n} = 3$, $\theta = 3\pi/4$, and the other parameters as $(\mu, \chi) = (1, 1)$

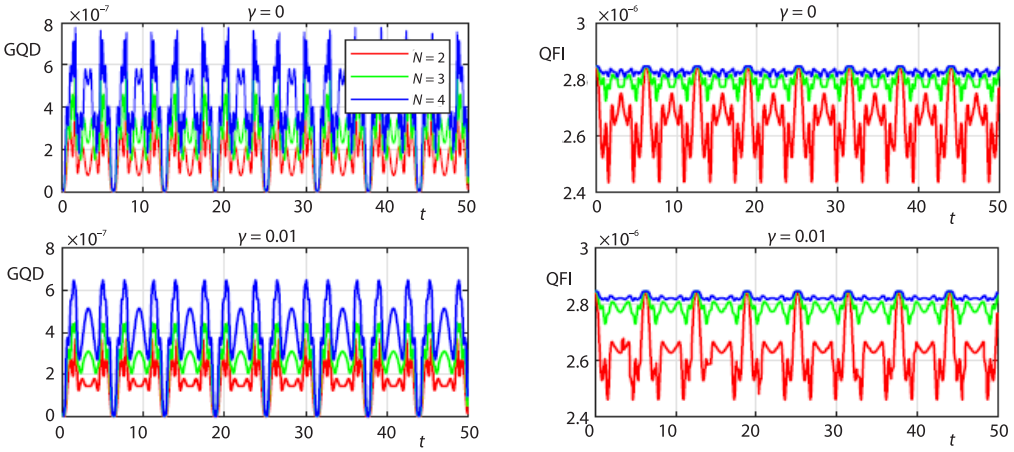

Figure 6. The dynamics of the quantifiers are shown in the figure; we have chosen the parameters $\bar{n} = 3$, $\theta = 3\pi/4$, and the other parameters as $(\mu, \chi) = (1, 3)$

sistent across N. Under $\gamma = 0.01$, QFI shows no significant decay across N values. In the case of $\chi = 3$, GQD and QFI maintain periodic oscillations for both γ conditions. While GQD oscillation amplitude grows with N, QFI amplitude decreases as N increases. For $\gamma = 0.01$ with $\chi = 3$, GQD values decline relative to $\gamma = 0$, while QFI values remain unaffected by intrinsic decoherence in this case.

In comparing fig. 4 through fig. 6, the oscillation period for both GQD and QFI remains consistent despite changes in χ. The GQD values decrease as χ increases, whereas QFI values improve with higher χ. Additionally, the amplitude of oscillations for both GQD and QFI reduces with increasing χ, with the most significant decrease observed at $\chi = 3$ for $N = 4N$. We examine how varying the average thermal photon number influences system dynamics. Figure 7 presents the evolution of GQD and QFI for initial average thermal photons, with $|\alpha|^2$ set at 4 and 5. Parameters are chosen as $N = 2$, $\chi = 1$, $p = 0.5$, and $\theta = 3\pi/4$. As the average thermal photon number increases, both GQD and QFI values display suppressed dynamics, along with a decrease in their oscillation amplitude. Notably, the GQD values remain unaffected by intrinsic decoherence when the average thermal photon number changes. In contrast, the QFI value decreases with intrinsic decoherence for $|\alpha|^2 = 4$, while it remains stable for $|\alpha|^2 = 5$.

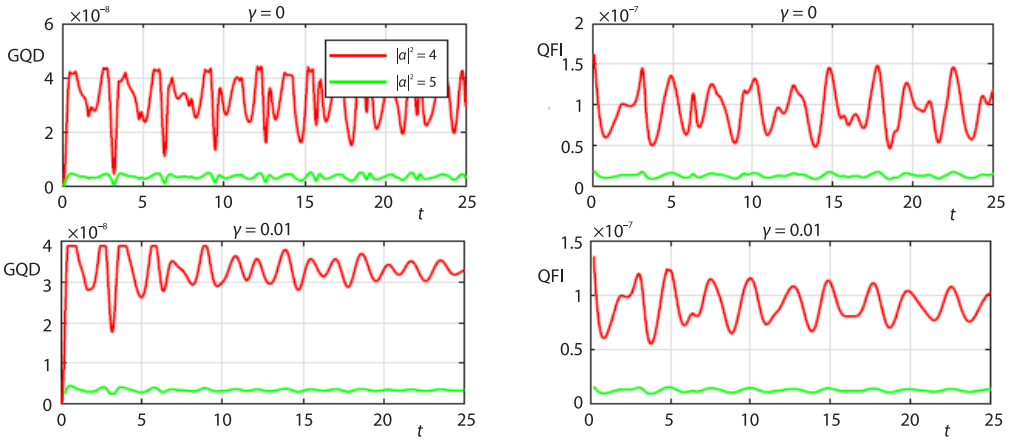

Figure 7. The GQD and QFI's dynamic behavior under the situation of two distinct average thermal photons; we have taken $|\alpha|^2 = 4$ and 5, $\theta = 3\pi/4$, $p = 0$, and $\chi = 0.3$

Conclusion

In recent years, there has been a great deal of interest in the study of the evolution of multipartite quantum correlations and entanglement in open quantum systems interacting with the environment and in more realistic cavity circumstances. We have examined the multipartite quantum correlations and the entanglement of systems comprising N-TLS due to their potential application in the development of quantum information. This work has discussed the time evolution of GQD and QFI for multiple-TLS interacting with a single-mode thermal field and an NLKM. We examined the dynamics of the GQD and QFI for two, three, and four TLS in motion, both with and without intrinsic decoherence. We found that, by keeping the parameter the same, the GQD and QFI values increased by increasing N for both γ cases. The GQD values of the system decreased with an increase in χ. The rapidness of oscillation of the GQD also increased with an increase in χ. In the presence of intrinsic decoherence, the GQD quasi-static value did not reduce with respect to the average value it without intrinsic decoherence for χ = 0.3 and χ = 1 cases. However, we observed a reduction in the quasi-steady value of the GQD for χ = 3 as compared to the zero decoherence case. The QFI average value increases for the system if χ value is increased. The fluctuating amplitude decreased by increasing χ. For the larger N subsystems, the amplitude of oscillation of the QFI has a further increasing. Unlike the GQD case, larger χ values assisted and maintained the average QFI value in the presence of intrinsic decoherence. For the case of the moving atomic system, the period of oscillations of the GQD and QFI did not change by changing χ. For the moving system case, the values of the GQD decreased with the increase in χ. Whereas the QFI improved with the increase in χ. We observed that by increasing the average thermal photons inside the system, the value of the GQD and QFI was suppressed in the dynamics. The amplitude of oscillation of the GQD and QFI diminished with an increase in the average thermal photons.

Acknowledgment

The authors extend their appreciation Taif University, Saudi Arabia, for supporting this work through Project No. (TU-DSPP-2024-08)

References

[1] Buluta, I., *et al*., Natural and Artificial Atoms for Quantum Computation, *Rep. Prog. Phys*., *74* (2011), 104401

[2] Kim, M. S., *et al*., Entanglement induced By A Single-Mode Heat Environment, *Phys. Rev. A*, *65* (2002), 04010
[3] Zhang, B., Entanglement between Two Qubits Interacting with a Slightly Detuned Thermal Field, *Opt. Commun*., *283* (2010), 23, pp. 4676-4679
[4] Zhou, L., Song, H. S., Entanglement Induced by a Single-Mode Thermal Field and the Criteria for Entanglement, *J. Opt. B: Quantum Semiclass. Opt*., *4* (2002), 425
[5] Bashkirov, E. K., Entanglement Induced by the Two-Mode Thermal Noise, *Laser Phys. Lett*., *3* (2006), 145
[6] Aguiar, L. S., *et al*., The Entanglement of Two Dipole-Dipole Coupled Atoms in a Cavity Interacting with a Thermal Field, *J. Opt. B: Quantum Semiclass. Opt.*, *7* (2005), S769
[7] Bashkirov, E. K., Stupatskaya, M. P., The Entanglement Of Two Dipole-Dipole Coupled Atoms Induced by Non-Degenerate Two-Mode Thermal Noise, *Laser Phys*., *19* (2009), Mar., pp. 525-530
[8] Jaynes, E. T., Cummings, F. W., Comparison of Quantum and Semiclassical Radiation Theories with Application the Beam Maser, *Proc. IEEE*, *51* (1963), 1, pp. 89-109
[9] Liu, Z. D., *et al.*, The Properties of a Light Field Interacting with a Four-Level Atom, *J. Mod. Opt*., *45* (1988), 5, pp. 833-842
[10] Liu, X., Entropy Behaviors And Statistical Properties of the Field Interacting with a Ξ-Type Three-Level Atom, *Physica A*, *286* (2000), 3-4, pp. 588-598
[11] Abdel-Khalek, S., Nofal, T. A., Correlation and Entanglement of a Three-Level Atom Inside a Dissipative Cavity, *Physica A*, *390* (2011), 13, pp. 2626-2635
[12] Eleuch, H., *et al.*, Effects of an Environment on a Cavity-Quantum-Electrodynamics System Controlled by Bichromatic Adiabatic Passage, *Phys. Rev. A*, *85* (2012), 013830
[13] Abdel-Aty, A., *et al*., Entanglement and Teleportation Via a Partial Entangled-State Quantum Network, *J. Comput. Theor. Nanosci.*, *12* (2015), 9, pp. 2213-2220
[14] Bennett, C. H., DiVincenzo, D. P., Towards an Engineering Era, *Nature*, *377* (1995), Oct., pp. 389-390
[15] Cirac, J. I., Zoller, P., A Scalable Quantum Computer with Ions in an Array of Micro Traps, *Nature*, *404* (2000), Apr., pp. 579-581
[16] Divincenzo, D. P., Quantum Computation, *Science*, *270* (1995), Oct., pp. 255-261
[17] Grover, L. K., Quantum computers Can Search Arbitrarily Large Databases by a Single Query, *Phys. Rev. Lett*., *79* (1997), 4709
[18] Yin, Z.-Q., *et al.*, Security of Counterfactual Quantum Cryptography, *Phys. Rev. A*, *85* (2010), 042335
[19] Noh, T. G., Counterfactual Quantum Cryptography, *Phys. Rev. Lett*., *103* (2009), 230501
[20] Louisell, W. H., *et al*., Quantum Fluctuations And Noise In Parametric Processes, *Phys. Rev*., *124* (1961), 1646
[21] Bennett, C. H., DiVincenzo, D. P., Quantum information and Computation, *Nature*, *404* (2000), pp. 247-255
[22] Abdel-Khalek, *et al.*, Effect of time Dependent Coupling on the Dynamical Properties of the Non-Local Correlation between Two Three-Level Atoms, *International Journal of Theoretical Physics*, *56* (2017), June, pp. 2898-2910
[23] Abdalla, M. S., Nassar, M. M., Quantum Treatment of the Time-Dependent Coupled Oscillators under the Action of a Random Force, *Ann. Phys*., *324* (2009), 3, pp. 637-669
[24] Korashy, S.T., *et al*., Dynamics of a Non-Linear Time-Dependent Two Two-Level Atoms in a Two-Mode Cavity, *Int. J. Quantum Inf*., *18* (2020), 2050003
[25] Korashy, S. T., *et al.*, Influence of Stark shift and Kerr-Like Medium on the Interaction of a Two-Level Atom with Two Quantized Field Modes: A Time-Dependent System, *Quant. Inf. Rev.. 5* (2017), 1, pp. 9-14
[26] Fisher, R. A., Theory of Statistical Estimation, *Proc. Cambridge Philos. Soc*., *22* (1925), 5, pp. 700-725
[27] Barndorff-Nielsen, O. E., Gill, R. D., Fisher Information In Quantum Statistics., *J. Phys. A: Math. Gen*., *33* (2000), 4481
[28] Giovannetti, V., *et al*., Quantum Metrology, *Phys. Rev. Lett*., *96* (2006), 010401
[29] Lu, X.-M., *et* al., Hierarchy of Measurement-Induced Fisher Information for Composite States, *Phys. Rev. A*, *86* (2012), 022342
[30] Milburn, G. J., Intrinsic decoherence in Quantum Mechanics, *Phys. Rev. A*, *44* (1991), 5401
[31] Henderson, L., *et al*., Quantum and Total Correlations, *J. Phys. A*, *34* (2001), 6899
[32] Ollivier, H., Zurek, W. H., Quantum Discord: A Measure of the Quantumness of Correlations, *Phys. Rev. Lett*., *88* (2002), 017901
[33] Rulli, C. C., Sarandy, M. S., Global Quantum Discord in Multipartite Systems, *Phys. Rev. A*, *84* (2011), 042109

[34] Modi, K., *et al*., Unified View of Quantum and Classical Correlations, *Phys. Rev. Lett*., *104* (2010), 080501
[35] Chakrabarty, I., *et al*., Quantum Dissension: Generalizing Quantum Discord for Three-Qubit States, *Eur. Phys. J. D*., *56* (2011), Dec., pp. 605-612
[36] Chen, L., *et a*l., Detecting Multipartite Classical States and Their Resemblances, *Phys. Rev. A*, *83* (2011), 020101(R)
[37] Berrada, K., *et al*., Quantum Metrology with Entangled Spin-Coherent States of Two Modes, *Phys. Rev. A*, *86* (2012), 033823
[38] Wootters, W. K., Entanglement of Formation and Concurrence, *Quantum Inf. Comput*., *1* (2001), 1, pp. 27-44
[39] Lu, X., *et al*., Quantum Fisher Information Flow and Non-Markovian Processes of Open Systems, *Phys. Rev. A*, *82* (2010), 042103
[40] Barndorff-Nielsen, O. E., *et al*., On Quantum Statistical Inference, *J. R. Stat. Soc. B*, *65* (2003), 4, pp. 775-816
[41] Tavis, M., Cummings, F. W., Exact Solution for an N-Molecule-Radiation-Field Hamiltonian, *Phys. Rev*., *170* (1968**)**, 379
[42] Schlicher, R. R., Jaynes-Cummings Model with Atomic Motion, *Opt. Commun*., *7*0 (1989), 2, pp. 97-102
[43] Guo J. L., Song H. S., Entanglement between two Tavis-Cummings Atoms with Phase Decoherence, *J. Mod. Opt*., *56* (2009), 4, pp, 496-501
[44] Campbell, S., *et al*., Global Quantum Correlations in Finite-Size Spin Chains, *New J. Phys*., *15* (2013), 043033

Paper submitted: July 13, 2024
Paper revised: September 30, 2024
Paper accepted: October 29, 2024